Electronic Supplementary Material (ESI) for New Journal of Chemistry.
This journal is © The Royal Society of Chemistry and the Centre National de la Recherche Scientifique 2020

Solid-state host-guest influences on a BODIPY dye hosted within a crystalline sponge

William J. Gee,[a]* Helena J. Shepherd,[b] Daniel M. Dawson,[c] Sharon E. Ashbrook,[c] Paul R. Raithby[d] and Andrew D. Burrows.[d]*

a) School of Environment and Science, Griffith University, 170 Kessels Road, Brisbane, QLD 4111, Australia. Email: W.Gee@griffith.edu.au.
b) School of Physical Sciences, University of Kent, Canterbury, Kent, CT2 7NH, United Kingdom.
c) School of Chemistry and EaStCHEM, University of St Andrews, North Haugh, St Andrews KY16 9ST, United Kingdom.
d) Department of Chemistry, University of Bath, Claverton Down, Bath, BA2 7AY, United Kingdom. Email: a.d.burrows@bath.ac.uk.

Supporting Information

* To whom correspondence should be addressed.
Email: a.d.burrows@bath.ac.uk Telephone: +44 (0) 1225 386529

Email: W.Gee@griffith.edu.au Telephone: +61 (0) 7373 55154

Table of Contents

1. Powder patterns of 1 and 1·BODIPY

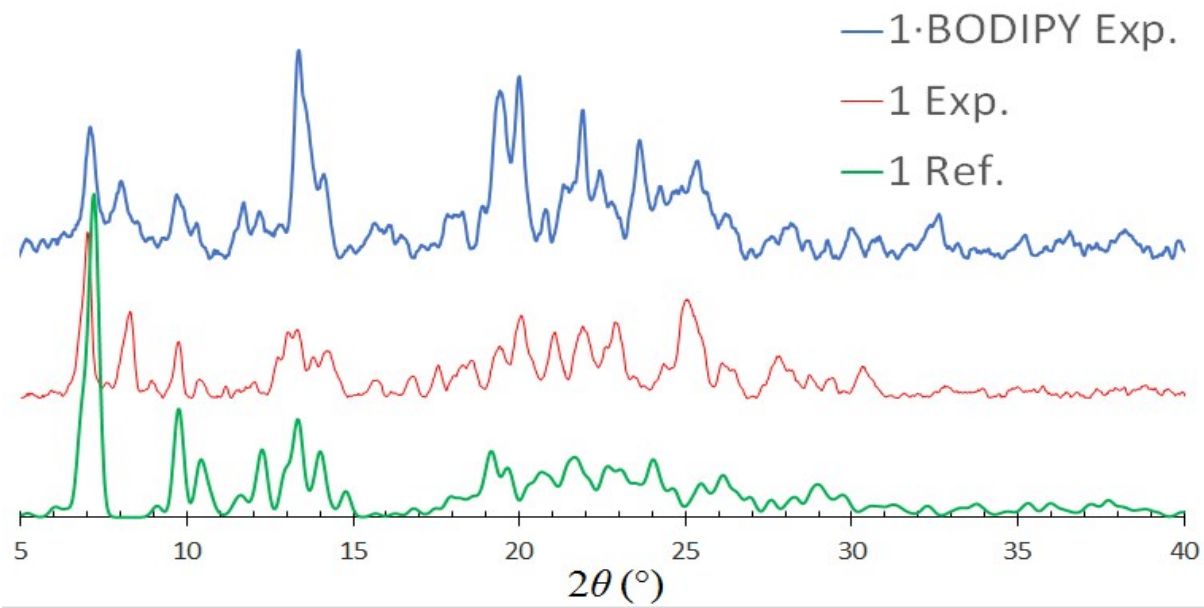

Fig. S1 Comparison of the PXRD profiles of experimental **1** (red), experimental **1**·BODIPY (blue), with a reference pattern (generated using Lazy Pulverix)[S1] for **1** (green) that was determined during this study at 150 K.

Crystal sponge frameworks are widely known to be highly flexible, which is a key reason why these materials have an affinity for hosting guests with a wide range of steric profiles. This flexibility poses a challenge for matching experimental powder patterns with their predicted patterns from single-crystal diffraction data. Variation in peak location and intensity at low angles can be attributed to the flexible nature of the framework upon solvent loss, coupled with differences in collection temperatures (150 K for single crystal data, 298 K for PXRD data). Studies have also reported that solvent exchange, which is a key aspect of activation and guest loading of crystalline sponges, can trigger phase transitions in these materials. This may justify the reduced quality of the PXRD patterns shown here.[S2-S4]

2. Comparison of PXRD pattern of crystalline BODIPY (guest) to 1·BODIPY (host)

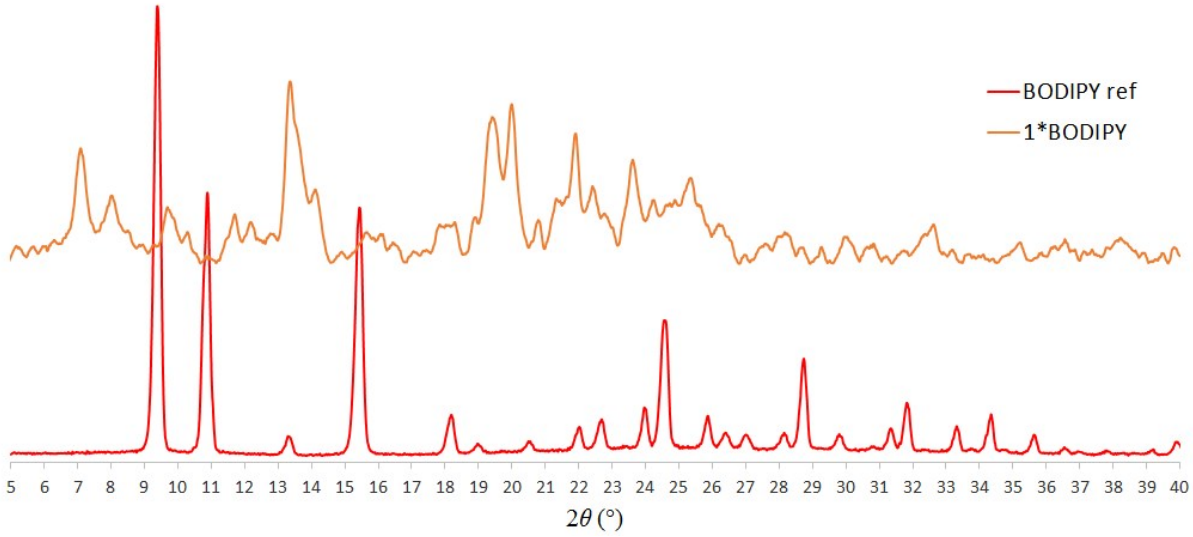

Fig. S2: No evidence of pure crystalline BODIPY (red trace) was observable in the PXRD pattern of **1**·BODIPY (orange trace), suggesting that the fluorescent emission observed derives from fluorophore located within the framework pores as opposed to forming a polycrystalline coating on the sample or a discrete mixture of each individual component.

3. IR Spectra of 1 and 1·BODIPY

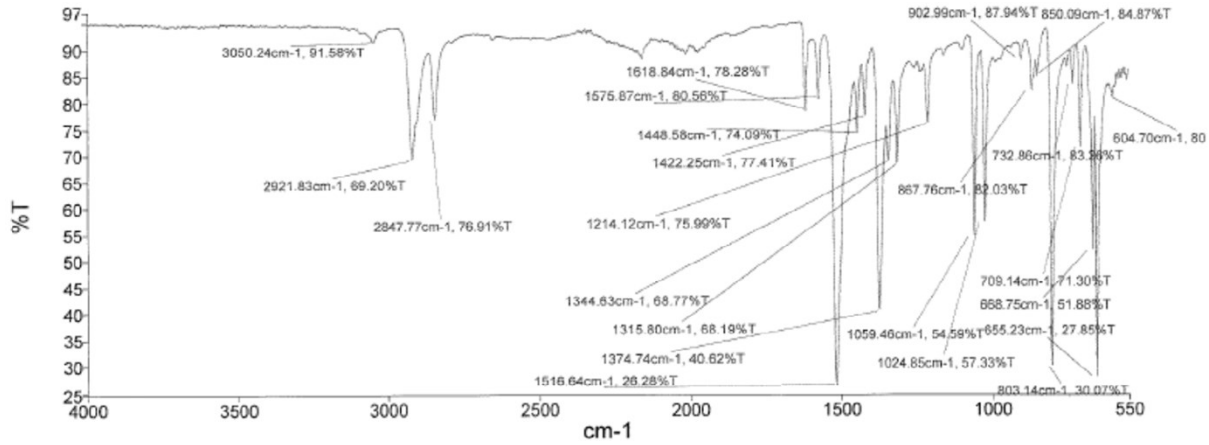

Fig. S3: IR spectrum of empty crystalline sponge **1**

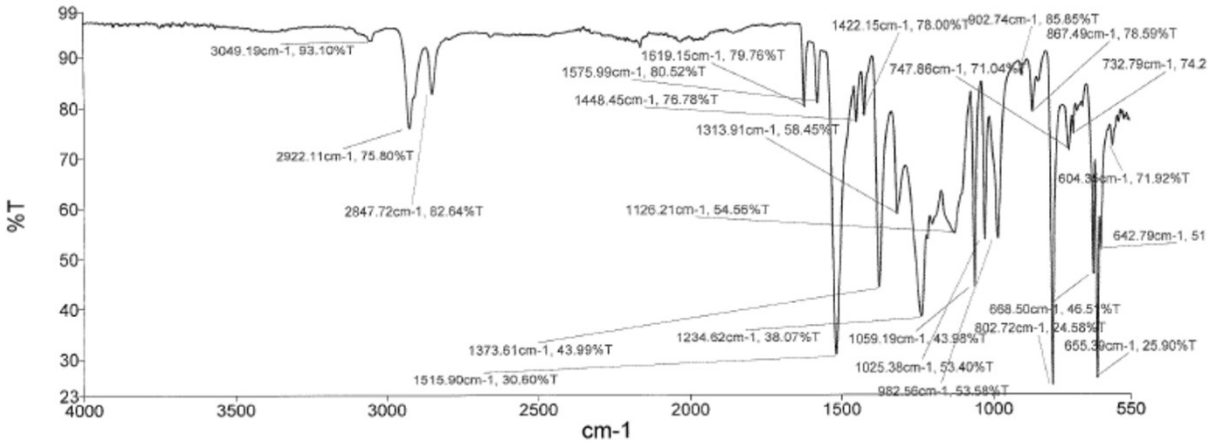

Fig. S4: IR spectrum of **1**·BODIPY

4. Crystallographic Summary

Table 1 Crystal data and structure refinement for 1·BODIPY.

Identification code	1·BODIPY
CCDC	1535880
Empirical formula	$C_{39}H_{30}I_6N_{12}Zn_3$
Formula weight	1624.26
Temperature/K	150.10(10)
Crystal system	monoclinic
Space group	C2/c
a/Å	35.2899(10)
b/Å	14.8461(3)
c/Å	32.3685(9)
α/°	90
β/°	103.634(3)
γ/°	90
Volume/Å^3	16480.5(8)
Z	8
ρ_{calc}g/cm^3	1.309
μ/mm^{-1}	18.867
F(000)	6048.0
Crystal size/mm^3	0.1785 × 0.101 × 0.0678
Radiation	CuKα (λ = 1.54184)
2Θ range for data collection/°	6.488 to 117.862
Index ranges	-39 ≤ h ≤ 36, -15 ≤ k ≤ 16, -35 ≤ l ≤ 35
Reflections collected	29531
Independent reflections	11822 [R_{int} = 0.0325, R_{sigma} = 0.0318]
Data/restraints/parameters	11822/152/550
Goodness-of-fit on F^2	1.443
Final R indexes [I>=2σ (I)]	R_1 = 0.0953, wR_2 = 0.3218
Final R indexes [all data]	R_1 = 0.1064, wR_2 = 0.3443
Largest diff. peak/hole / e Å^{-3}	2.06/-1.86

5. Residual electron density map of 1·BODIPY

Experimental details

The electron density map of **1·BODIPY** was generated from single crystal X-ray data obtained with an Agilent SuperNova using Cu(Kα) radiation. The analysis was conducted at 150 K. The structure was solved using SHELXS-97 and refined using full-matrix least squares in SHELXL-97.[S5] The electron density map was generated using Olex2.[S6] Despite the crystals diffracting well when irradiated with X-rays, the BODIPY guest did not exhibit a degree of ordering within the pores of the crystalline sponge that allowed unambiguous assignment of its structure. Consequently, the obtained crystal data offers no insight beyond the previously reported crystalline sponge examples, and is therefore not reported here beyond discussion of the electron density map below.

Further discussions quantifying the BODIPY guest

The unit cell obtained from crystalline BODIPY was matched to a known crystal structure in which columnar stacks of fluorophore pack in an antiparallel manner, maximising $\pi-\pi$ stacking between molecules.[S6] The unit cell for BODIPY is 1288 Å^3 and contains four close-packed molecules of the fluorophore, each occupying *ca*. 320 Å^3. In contrast, the unit cell volume of **1**·BODIPY is 16481 Å^3, which, accounting for formula units per cell, and the loading percentage of BODIPY (*i.e.* the ratio of 1 : 3.08 (BODIPY : tpt) determined with NMR spectroscopy), will contain 5.2 equivalents of fluorophore per unit cell. This equates to a percentage volume of fluorophore within unit cell of **1**·BODIPY of 10.2%, compared with 100% for pure crystalline BODIPY.[S7]

Residual electron density maps

A region of high residual electron density was observed in the difference map of the crystal structure of **1**·BODIPY, close to one of the tpt ligand molecules, as shown in Figures S5 & S6. While individual atomic positions could not be unambiguously determined for the BODIPY molecule, the size and location of the residual density are chemically sensible for the location of the guest molecule. The inability to assign atomic positions is perhaps unsurprising considering that the diffraction pattern will be dominated by scattering from heavy elements within the framework (iodine and zinc). Assignment of partially occupied (0.65 equivalents from NMR) and (potentially disordered) light-atom guest molecules from such data is not trivial.[S8]

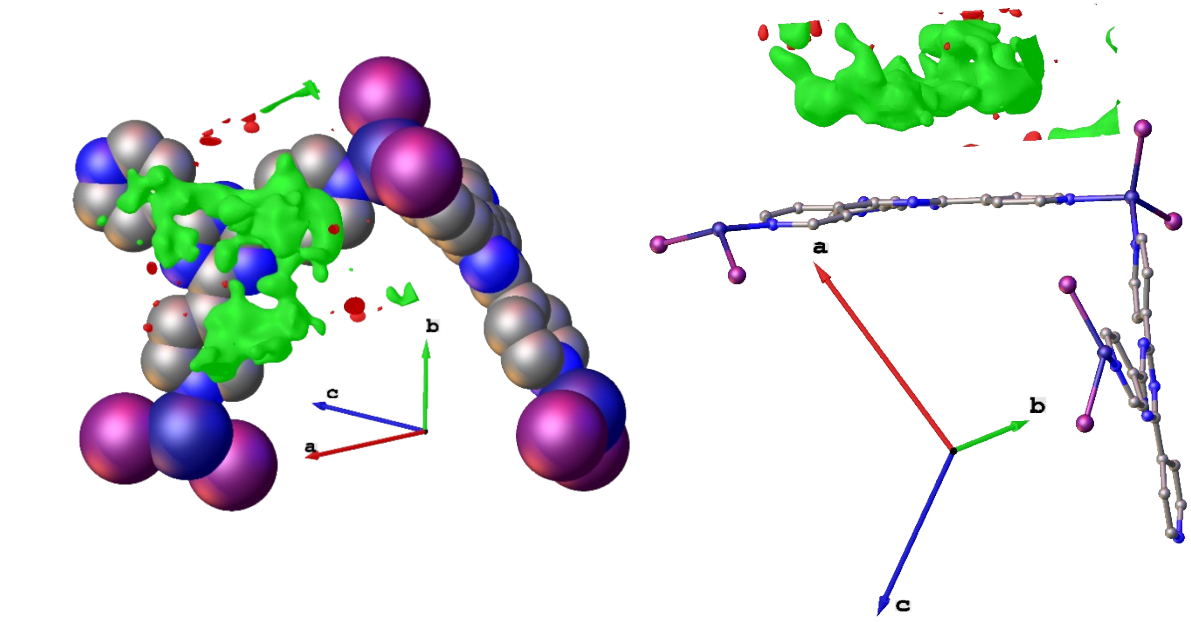

Fig. S5: Residual electron density map within the pore of **1**·BODIPY showing the probable location of the BODIPY guest. Atoms shown as spheres (C = grey, N = blue, I = pink, Zn = dark purple). Residual electron density greater than 1.1 e/Å is shown as green for positive, red for negative.

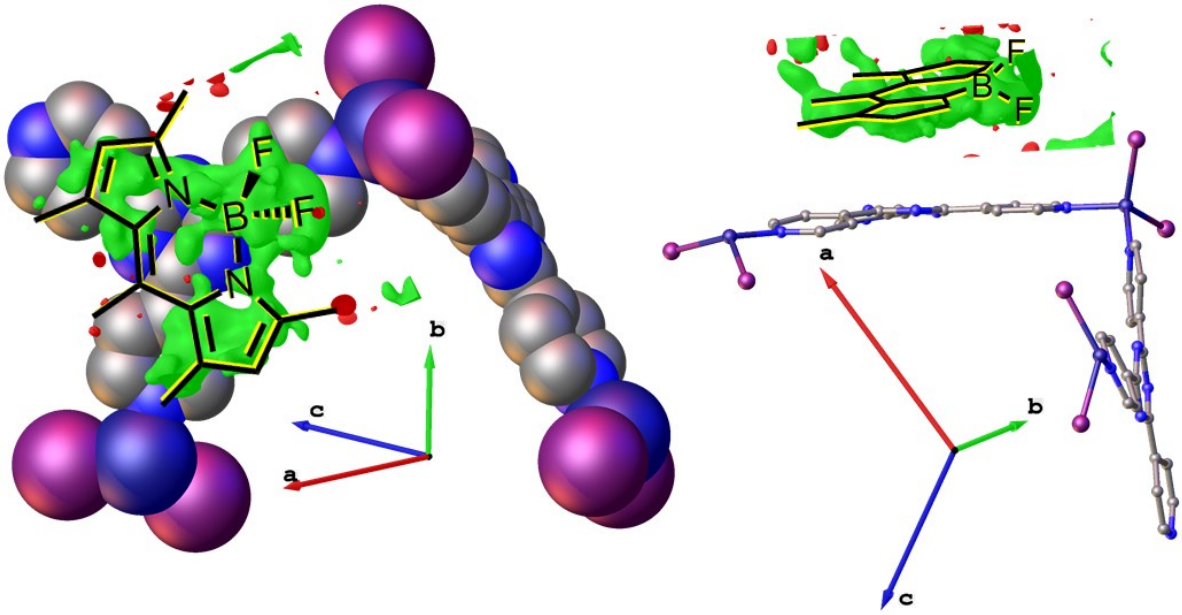

Fig. S6: Analogous residual electron density map to Fig. S5 showing the proposed location of BODIPY with a wireframe structure to guide the eye.

6. ^{1}H-NMR spectrum obtained from a digested single crystal of 1·BODIPY

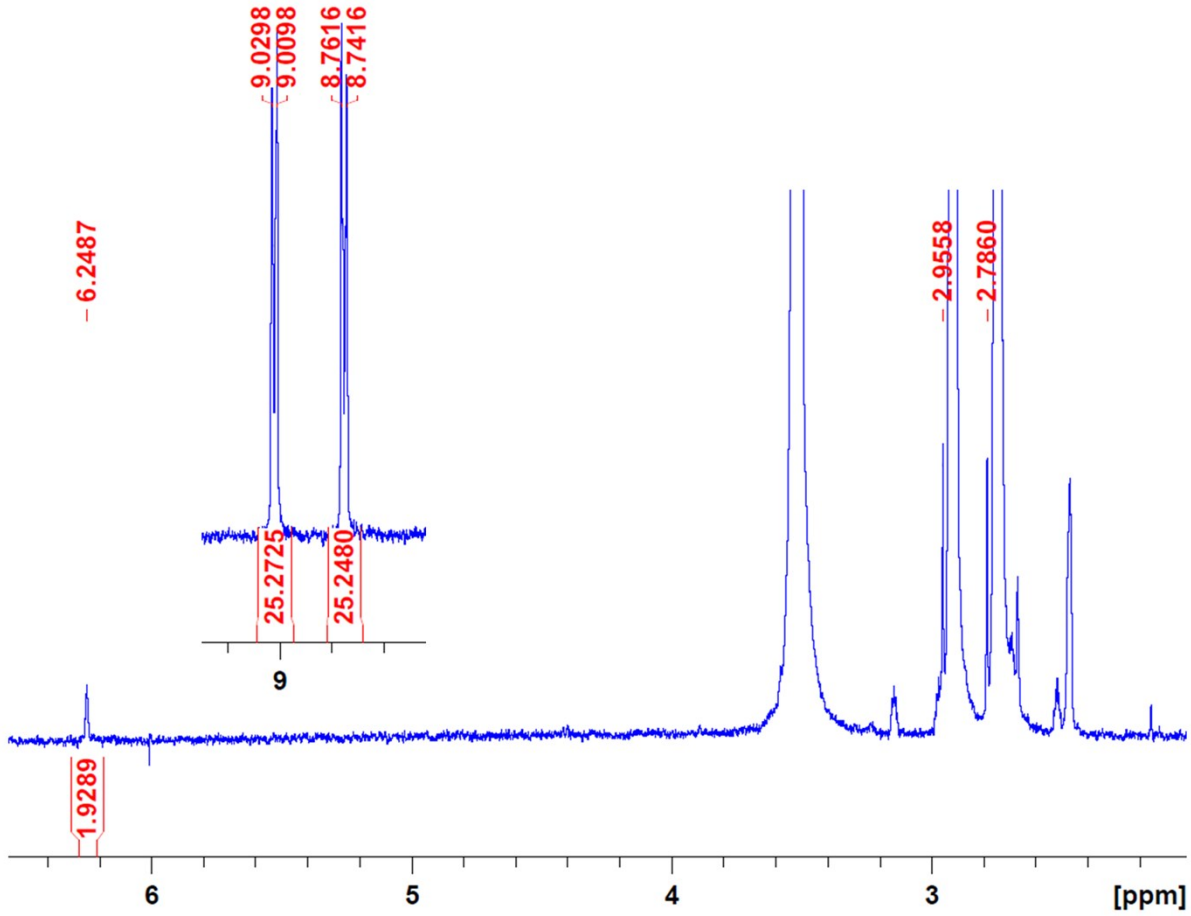

Fig. S7: The ^{1}H-NMR spectrum of an individual single crystal of **1**·BODIPY digested in DMF-d_7. Characteristic aromatic resonances of tpt are shown in the inset (ranging from 8.6 – 9.2 ppm). Pyrromethene resonances consistent with BODIPY and matching those reported in Figure 2 were also observed, with the exception of the methyl group at 3.57 ppm which here was obscured by a large signal attributed to a water peak. The integrals used to calculate the loading value for the single crystal sample are shown above, giving 1:4.36 (BODIPY:tpt), or 0.46 BODIPY per crystallographic formula unit of the single crystal.

7. ^{19}F NMR spectrum obtained from digested 1·BODIPY

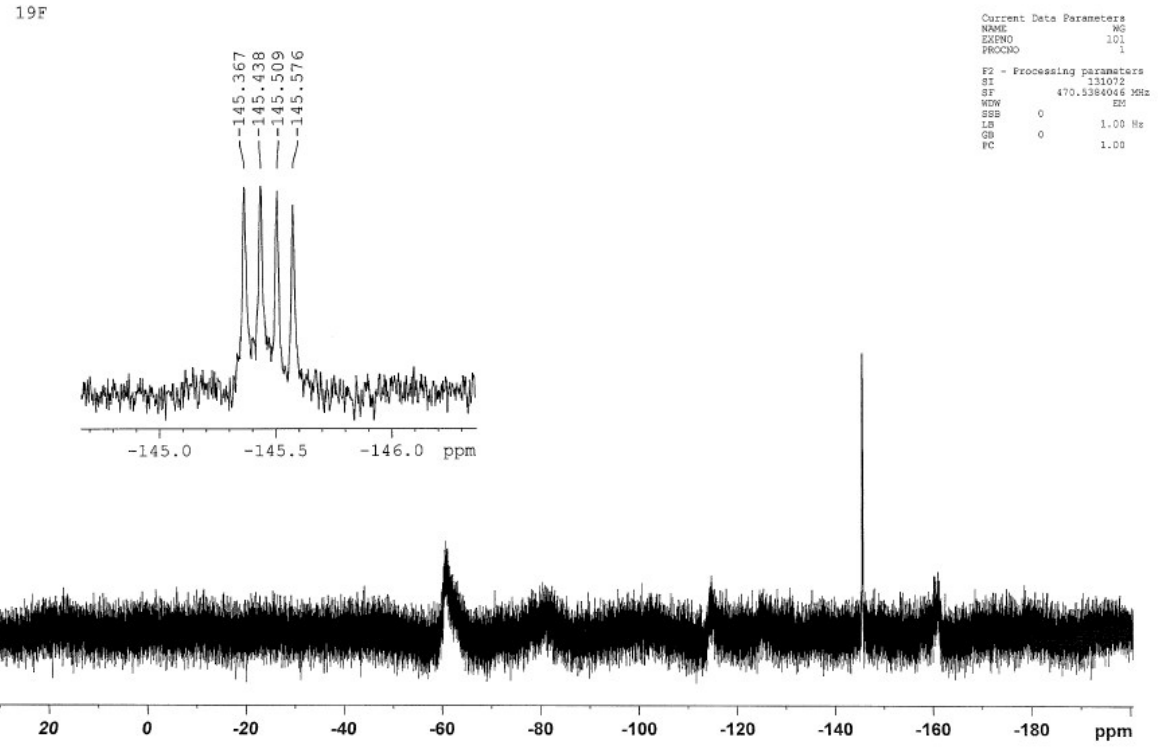

Fig. S8: ^{19}F-NMR spectrum obtained from digested **1**·BODIPY showing the sharp 1:1:1:1 quartet indicative of the BF_2 group of BODIPY.

8. Additional Solid-state NMR spectra

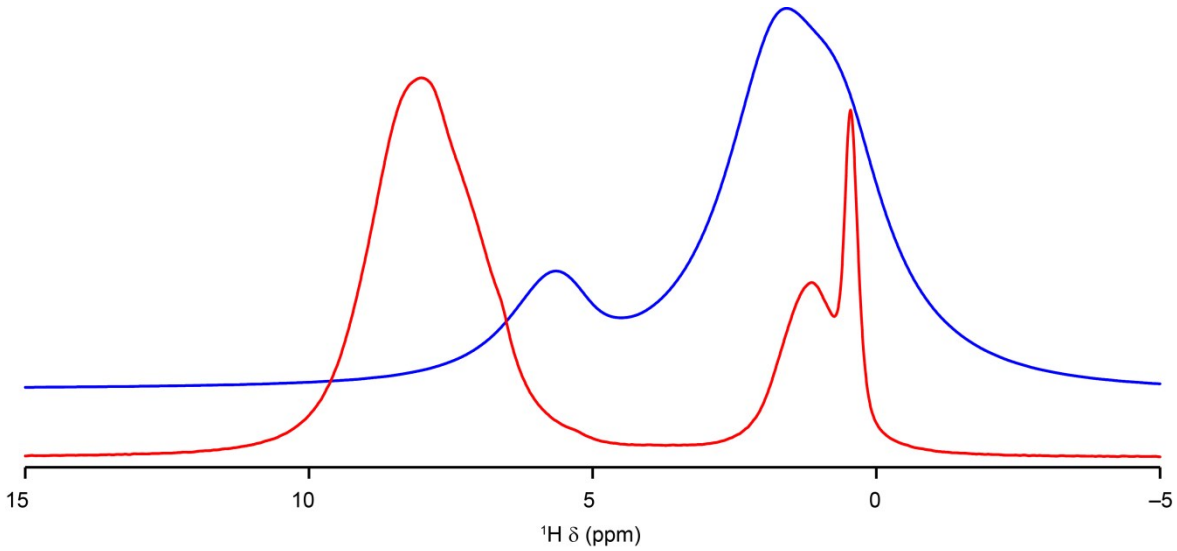

Fig. S9: ^{1}H (9.4 T, 40 kHz MAS) NMR spectra of BODIPY (blue) and **1**·BODIPY (red).

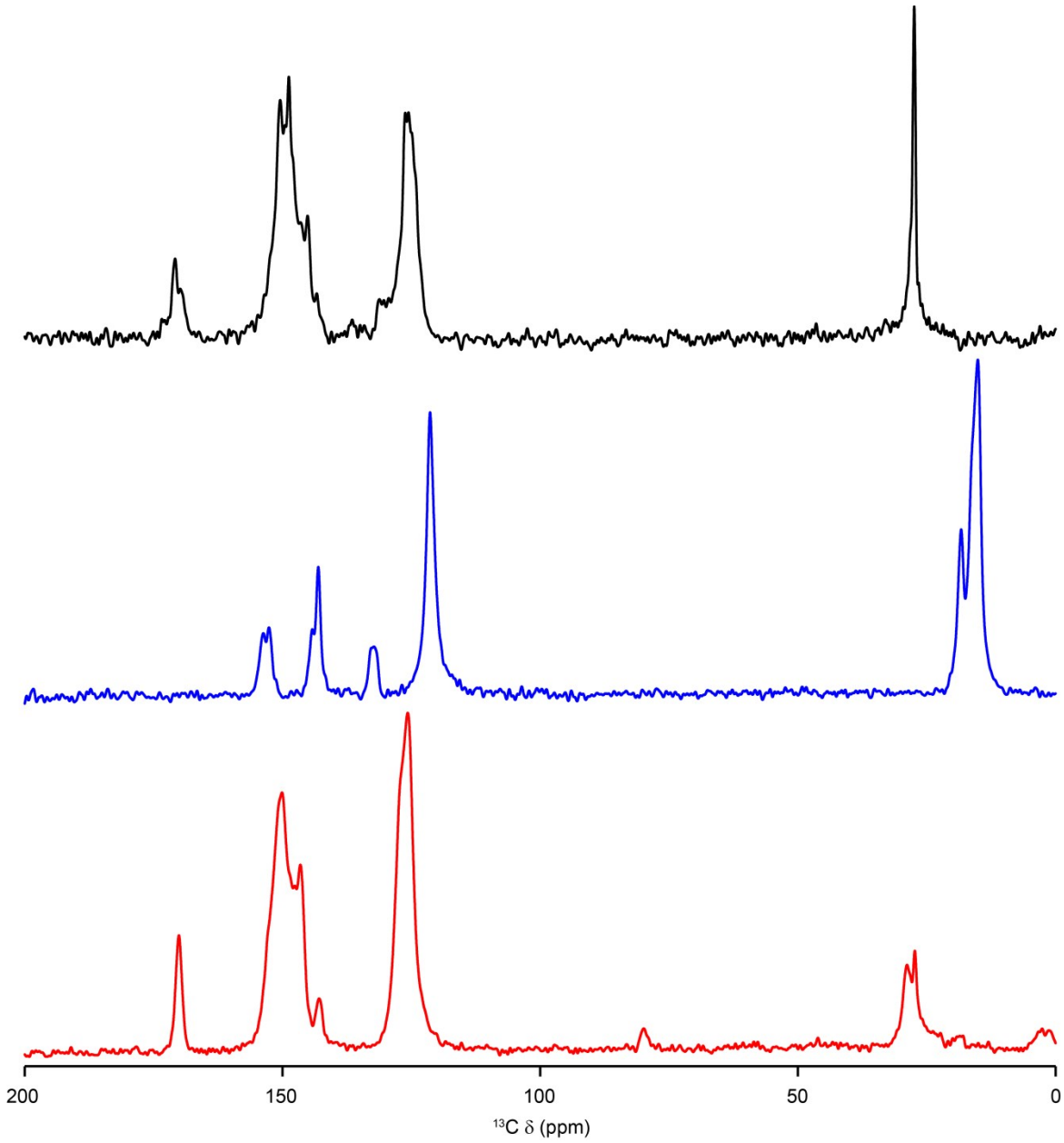

Fig. S10: ^{13}C (9.4 T, 12.5 kHz CPMAS) NMR spectra of **1** (black), BODIPY (blue) and **1**·BODIPY (red).

9. References

S1: K. Yvon, W. Jeitschko, E. Parthé, *J. Appl. Cryst.* **1977**, *10*, 73.

S2: H. Ohtsu, T. D. Bennett, T. Kojima, D. A. Keen, Y. Niwa, M. Kawano, *Chem. Commun.*, **2017**, *53*, 7060.

S3: K. Ohara, J. Martí-Rujas, T. Haneda, M. Kawano, D. Hashizume, F. Izumi, M. Fujita, *J. Am. Chem. Soc.* **2009**, *131*, 3860.

S4: J. Martí-Rujas, N. Islam, D. Hashizume, F. Izumi, M. Fujita, M. Kawano, *J. Am. Chem. Soc.*, **2011**, *133*, 5853.

S5: G. M. Sheldrick, *Acta Cryst.* **2008**, *A64,* 112.

S6: O. V. Dolomanov, L. J. Bourhis, R. J. Gildea, J. A. K. Howard, H. Puschmann, *J. Appl. Cryst.* **2009**, *42*, 339.

S7: S. Choi, J. Bouffard, Y. Kim, *Chem. Sci.* **2014**, *5*, 751.

S8: T. R. Ramadhar, S.-L. Zheng, Y.-S. Chen, J. Clardy, *Chem. Commun.*, **2015**, *51*, 11252.